ANALYSIS OF INTRINSIC VARIABILITY AND OUTLIERS IN PULSED NEUTRON DATA USING THE MARS SCIENCE LABORATORY DYNAMIC ALBEDO OF NEUTRONS INSTRUMENT H. R. Kerner[1], C. Hardgrove[1], S. Czarnecki[1], [1]School of Earth and Space Exploration, Arizona State University, 781 E. Terrace Mall, Tempe, AZ 85287, hkerner@asu.edu.

Introduction: The Dynamic Albedo of Neutrons (DAN) instrument onboard Mars Science Laboratory (MSL) *Curiosity* acquired ~900 active neutron measurements in Gale Crater between 08/06/2012 (sol 1) and 09/14/2018 (sol 2171). In active mode, DAN emits neutrons into the surface in discrete pulses (10 Hz) using a pulsed neutron generator (PNG). DAN measures the neutron albedo using two ^{3}He detectors (for thermal and epithermal neutrons, <0.3 eV and 0.3 eV-100 keV respectively) that bin counts into 64 lognormal time bins between pulses [1]. These time-resolved neutron data (called neutron "die-away" curves) are sensitive to the abundance of hydrogen, neutron absorbing elements as well as their depth distributions. MSL acquires neutron die-away measurements with DAN at the end of every drive and, less frequently, when requested by the science team. Thus, the DAN dataset represents a relatively unbiased and uniform sampling of the Gale Crater near-surface geochemistry along MSL's traverse. Example neutron die-away curves using a Gale Crater geochemistry (**Fig. 1**) demonstrate the effect of hydrogen (H) (in wt. %) and bulk neutron absorption cross section (Σ_{abs}; in barns, b) on neutron die-away [1]. These elements are important indicators for geologic processes on Mars, e.g., evaporitic mineral precipitation, acidic weathering, and aqueous alteration [3]. It is important to consider contextual and compositional geologic data when deriving H, Σ_{abs}, and their depth distributions from an active neutron experiment. Compared to orbital measurements (which are passive experiments), surface neutron measurement footprints are highly localized (e.g., a few meters in diameter underneath the lander/rover), and rock/soil compositions change as the rover moves from one location to the next [4].

Neutron die-away is a standard technique in the resource exploration industry first described for planetary science by Trombka et al. in 1968, who described trends in neutron die-away with mafic vs. felsic rocks [2]. More recently, Hardgrove et al. [3] modeled the expected variability that could be observed in neutron die-away due to changes in hydrogen (H) and neutron absorbing elements that would be expected at the Martian equator (Fe, Cl). To date, however, there has been no comprehensive study of the intrinsic variability in neutron die-away data. A formal understanding of how changes in H and Σ_{abs} manifest in neutron die-away data can help focus attention on the most important features and readily detect novel/unique measurements. We use a computational model of the DAN detector and PNG geometry with a basic Mars soil geochemistry derived from in situ measurements as a starting point for systematically understanding the variability in neutron die-away from a mounted surface platform. We also demonstrate a method for identifying measurements that have anomalous geochemistry.

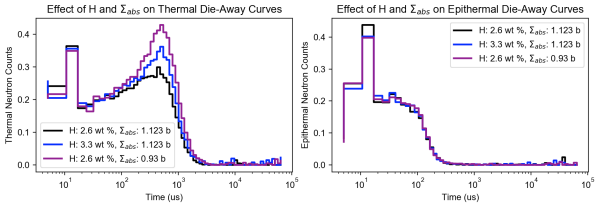

Figure 1 DAN data from sols 656 (blue), 668 (black), and 696 (purple). Interactions between neutrons and hydrogen in the subsurface result in increased thermal neutron counts (left, black vs. blue). Interactions between neutrons and neutron absorbers (Cl, Fe) result in decreased thermal neutron counts (left, black vs. purple). Epithermal neutron counts do not change significantly in either case (right).

MSL DAN Intrinsic Variability: We created a dataset of simulated measurements using a one-layer homogeneous model (including the MSL rover) varying H and Σ_{abs} in the subsurface over a range of values that might be observed in Gale Crater [5]. This resulted in 1,680 modeled measurements. We used principal component analysis (PCA) with three components to analyze the intrinsic variability in modeled neutron die-away measurements with varying H and Σ_{abs}. Three components explain 99.7% of the total variance in the modeled dataset and 96.7% in the DAN dataset.

Fig. 2 shows a contour plot illustrating how H and Σ_{abs} change along the first principal component (PC 1) and PC2 in the modeled dataset. The first component explains 93.7% of the variance in the dataset and PC2 explains 5.5%. These plots show that H *increases* (**Fig. 2** left) and Σ_{abs} *decreases* (**Fig. 2** right) non-linearly along PC1. **Fig. 2** (right) also shows that most of the principal subspace is spanned by low values of Σ_{abs}, indicating there is a large amount of variance between curves with low Σ_{abs}. **Fig. 3** shows how the shapes of the curves change along the principal axes, and thus what features are associated with each axis. **Fig. 3** (left) shows that the neutron die-away peak height is the most significant feature (PC1, row 1). Previous work showed thermal peak height is inversely correlated with Σ_{abs} and positively correlated with H [3]; we confirm this and further show this relationship is non-linear, i.e., the difference in peak height between curves with low values of H or Σ_{abs} is different than between curves with high values. **Fig. 3** (left, row 2) shows that an overall shift to earlier neutron arrival times is the second-most

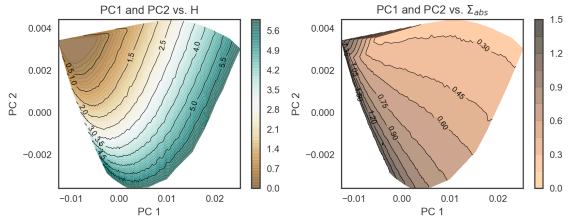

Figure 2 Contour plot illustrating changes in H (left) and Σ_{abs} (right) with PC1 and PC2 in modeled dataset.

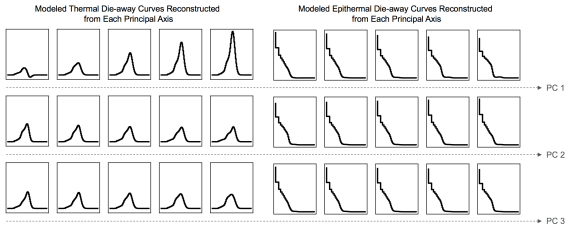

Figure 3 Thermal (left) and epithermal (right) neutron die-away curves along the first, second, and third principal axes of the modeled data set.

significant feature (PC2). Prior work showed this feature is a better metric than peak height for comparing water content between measurements [3]. The "roundness" of the peak is also significant (PC3), but has not been well-studied. **Fig. 3** (right) shows some change in convexity of epithermal curves along PC1, but no significant change along the other axes. This is consistent with prior work that showed there is minimal variation in epithermal neutron die-away counts with changes in hydration and Σ_{abs} (e.g., [3]).

Hardgrove et al. [3] showed that neutron die-away curves are sensitive to neutron absorbers in addition to H. Our observations suggest that when H is relatively low and invariant, e.g., in equatorial regions of Mars, thermal neutron die-away curves are primarily sensitive to changes in the abundance of neutron absorbing elements (primarily Fe and Cl). At polar latitudes, or where near-surface H-rich material (ice) may be present and more locally variable, neutron die-away may be primarily sensitive to bulk H content in the top ~50 cm (likely shallower) rather than Σ_{abs}. We will test this hypothesis in future work using modeled data from [3].

MSL DAN Measurements in Modeled Subspace. We projected our dataset of 895 DAN measurements onto the principal subspace of the modeled data. **Fig. 4** (left) shows the DAN data plotted together with the modeled data in this space. In **Fig. 4** (right), we colored *model* points red that best matched a DAN measurement. The DAN data are primarily clustered around the center of the subspace where we observed moderate H and Σ_{abs}.

MSL DAN Outlier Observations Along Traverse: To identify outliers in the DAN dataset, we performed PCA on measurements collected between sol 1-2171 and projected the data onto the principal subspace (**Fig. 5**, left). We computed the mean and standard deviation (σ) along each principal axis and considered all points $> 2\sigma$ from the mean to be outliers. We found the mean Σ_{abs} is significantly lower in the

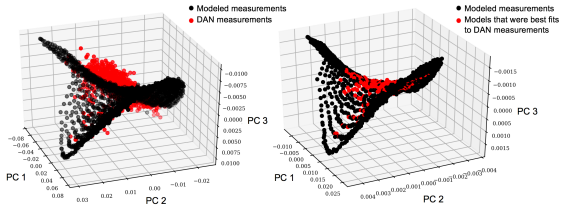

Figure 4 Left: DAN data set (red) projected into principal subspace of the modeled data set (black). Right: Modeled data set in principal subspace. Points that best fit a DAN measurement are colored red.

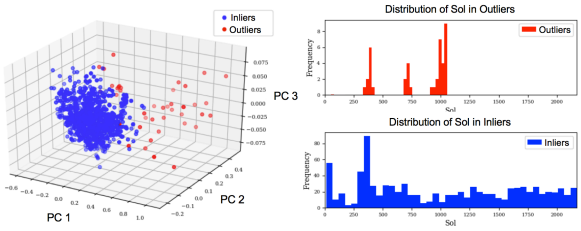

Figure 5 Left: DAN measurements projected onto principal subspace. Outlier points shown in red, inliers in blue. Right: histogram of sol on which measurements from (left) were acquired.

outlier population while the mean H content is similar in both populations. We found that while the sol (and thus location) distribution of inliers is uniform, the outliers occur in three distinct regions spanning sols 337-409, 690-744, and 924-1056 (**Fig. 5**, right). In the first two regions, felsic igneous rocks (low Fe) [6-7] and fracture-associated halos with elevated silica (high SiO_2, low Fe) [8] were observed by ChemCam and other MSL instruments. The third region is in Marias Pass (sols 992-1066) where a high-silica layer was observed ([9-10]). Interpretation of these outliers with respect to the geology of Gale Crater is ongoing.

Currently, to interpret data from DAN, modeling grids are generated to simulate neutron die-away with variable geochemistry and depth distributions. These simulations are then compared to the DAN data for each measurement [11]. This is important for placing data in the proper geologic context, but is not amenable to tactical planning timelines (e.g., the MSL science team has <12 hours for planning). As MSL continues using DAN to sample the subsurface in Gale Crater, we can use this method to quickly identify geochemical anomalies in the subsurface to guide follow-up studies. Additionally, this work demonstrates how active nuclear spectroscopy can be used to characterize the composition and distribution of hydrogen within the shallow subsurface (~top meter) of planetary surfaces and will be important for future missions that include active neutron investigations.

References: [1] Mitrofanov I. et al. (2012) *Space Science Reviews, 170(1-4),* 559–582. [2] Trombka J. I. and Schmadebeck R. L. (1968) *Nucl Instrum Methods, 62(3),* 253-261. [3] Hardgrove C. et al. (2011) *NIMA, 659*, 442–455. [4] Sullivan D. L. et al. (2019) *LPSC*. [5] Gabriel et al. (2018) *GRL*. [6] Sautter V. et al. (2014) *LPSC*. [7] Bridges J. C. (2016) *LPSC*. [8] Yen A. S. (2017) *EPSL, 471*, 186-198. [9] Czarnecki S. et al. (2019) *LPSC*. [10] Frydenvang J. et al. (2017). *GRL, 44(10),* 4716-4724. [11] Sanin et al. (2015) *NIMA, 789*, 114–127.